



# Study on Preparation and Adsorption Properties of Diatomite-Based Porous Ceramsite

Ruqin Gao<sup>†</sup>, Yiming Gu, Guoting Li and Qian Sun

School of Environmental and Municipal Engineering, North China University of Water Resources and Electric Power, Zhengzhou 450045, China

<sup>†</sup>Corresponding author: Ruqin Gao

Nat. Env. & Poll. Tech.  
Website: [www.neptjournal.com](http://www.neptjournal.com)

Received: 27-01-2017  
Accepted: 03-04-2017

## Key Words:

Diatomite-based porous  
ceramsite  
Adsorption  
Copper

## ABSTRACT

Using diatomite as the main material, diatomite-based porous ceramsite was prepared by wet grinding, molding by rolling and high-temperature calcinations. The structure and properties were characterized by X-ray diffraction, Scanning Electron Microscope, Mercury Injection Apparatus and so on. The ultraviolet-visible spectrophotometer was used to analyse the adsorption properties of diatomite-based porous ceramsite on  $\text{Cu}^{2+}$ . The results show that the pore size distribution of materials is 300–3500 nm, the specific surface area is 6.14  $\text{m}^2/\text{g}$ , and the pore porosity is 47.8%. Plenty of unsaturated bonds, such as -OH, Si-O-Si and O-Si-O, cluster on the surface of ceramsite. The removal rate of  $\text{Cu}^{2+}$  reaches 92.5%.

## INTRODUCTION

The diatomite forming from the debris of diatoms, microorganism and plants etc., by depositing in oceans and lakes is a kind of nonmetallic minerals. The diatomite has been widely used in water treatment technology because of its advantages such as acid-resisting, porous, large specific surface area and good adsorption (Annagiev et al. 2012, Ivanov et al. 2008, Liu et al. 2013, Zheng et al. 2014). But in practical application, diatomite powder causes blockage easily, so it is difficult to realize the dynamic adsorption. For the static treatment, there are some problems such as the difficulty for solid-liquid separation and regeneration, secondary pollution and so on. Using original pore structure of the diatomite and the pores by particles accumulating and pore-forming agent, porous ceramsite with different aperture and outstanding performance can be prepared (Simonenko et al. 2015, Gao et al. 2008).

With the development of mining, metallurgy, electroplating, electronics and other industries, heavy metal wastewater pollution is becoming more and more serious. In the waste-water discharge, heavy metal waste-water accounts for 60%, which is one of the largest water pollution hazards. However, cupric ion widely exists in industrial waste-water such as machine manufacturing, smelting, organic synthesis, metal processing and so on. When copper content in the water is greater than 3.0 mg/L, it has got obvious peculiar smell. When copper content is more than 15 mg/L, the water

cannot be drunk directly (Sun et al. 2003). As excessive copper entering the body and depositing in important organs such as liver, kidney etc., Wilson's disease may arise. The excess copper damages haemoglobin and the cell membrane, the activity of some enzymes will be suppressed, the normal metabolism of the body will be affected, and all this leads to diseases of the cardiovascular system (Chung 1996). In this paper, using diatomite as a raw material, diatomite based porous ceramsite (DBPC) with small aperture, good adsorption performance, low cost and easy recycle was prepared. The microstructure of the materials and its adsorption performance for copper ion was investigated.

## MATERIALS AND METHODS

**Material and reagent:** The diatomite powder was produced by Linjiang Beifeng Diatomite Co. Ltd. in Jilin Province. The grain diameter of the powder is 8.9  $\mu\text{m}$ , the pore diameter is 50-800 nm, and the specific surface area is 19.68  $\text{m}^2/\text{g}$ . The mass fraction of  $\text{SiO}_2$  is 82.54% in diatomite, the sintering aids of commercial pure include kaolin, quartz and feldspar, and the dispersant of analytic pure is the sodium silicate.

**Sample preparation and characterization:** The diatomite, sintering additives, the pore-forming agent and the dispersant were mixed with the mass ratio of 83:11:5:1, and then milled using water as zirconia balls (material:water:ball=1:2.5:1.8). After the obtained slurry was dried at 110°C, the powder was smashed, molded (the ball-forming machine), and sintered at 1140°C for 2 h.

Differential-thermal and thermal-gravimetric analysis (DTA-TG, Diamond, America) were examined on samples heated at 20°C/min up to 1080°C. The morphology of the as-prepared samples was examined by scanning electron microscopy (SEM, JSM-6490LV, Japan). The Fourier transform infrared spectrum was determined by Fourier transform infrared spectrum (FT-IR, BIO-RAD FTS 3000, America). The pore size distribution and the surface area etc. of the samples were investigated with mercury-injection apparatus (Auto Pore IV 9500, American). Referring to the national standard (GB1966-80), the porosity of the sample was analysed.

**Adsorption experiment of DBPC to Cu<sup>2+</sup>:** In this experiment, the adsorbents (1, 2, 4, 5, 10, 15 g/L) were added to the Cu<sup>2+</sup> solution (20 mg/L, 100 mL) under the condition of room temperature. Then, the adsorbents were vibrated in the constant temperature shaker for 120 min, taken out and filtered by microporous membrane. The chromogenic reagent was added to the aforesaid solution and water bath for 10 min in constant temperature (50°C), and then cooled to ambient temperature. According to the spectrophotometric method (the determination of copper ions adopts double acetaldehydes oxalyl two hydrazones spectrophotometry) and using distilled water as the reference, the absorbance of samples was measured in the maximum wavelength of 546 nm. On the basis of Lambert-Beer's law, there is a linear relation between the absorbance of samples in the maximum wavelength and its concentration. On the basis of the following equation, the removal rate for copper ion can be calculated.

$$\eta = \frac{A_0 - A_t}{A_0} \times 100\% \quad \dots(1)$$

Where,  $\eta$  represents the removal rate of the solution;  $A_0$  represents the initial absorbance in the solution,  $A_t$  represents the absorbance at time  $t$ .

## RESULTS AND DISCUSSION

**DTA-TG analysis of sample:** The DTA-TG curves of DBPC are shown in Fig.1 (the DTA curve is "a" curve, the TG curve is "b" curve). As shown from the figure, there are two stages of the physical changes in the process of DBPC heated from room temperature to 1050°C. In the first phase from room temperature to 600°C, specimens absorb plenty of

heat. At this stage, except the external and capillary water were removed, the chemical combined water and the organic matter in the rough-body were dislodged. This stage has the mass loss about 20%. In the second stage with the presence of oxygen, the carbon powder in the raw material was oxidized to CO<sub>2</sub>. The carbon powder was oxidized forming CO<sub>2</sub>, and the crystallization water was removed, so this reaction belonged to the exothermic reaction. In this stage, the thermogravimetric curve shows that the mass loss is about 6%.

**The microstructure of DBPC:** SEM image of DBPC is shown in Fig. 2. As seen from the image, the diatomite original pores and the holes from the particle accumulation constitute an organic whole. The tiny holes in diatomite disappeared, and the pores about 200~800 nm in the particles were retained. The small particles and the disc particles accumulated to form larger gaps. The number of three-dimension porosity composites organic integrity among the particles. This structure makes the specific surface area of the materials improve, and also makes the adsorption capacity of the materials on material surface to enhance.

**FT-IR analysis of sample:** Fig. 3 is the FT-IR spectrum of DBPC. As can be seen from the figure, there are many absorption peaks about OH- groups on the surface of DBPC (3451.30 cm<sup>-1</sup>, 1640.79 cm<sup>-1</sup>). Moreover, the peak intensity is evident, which specifies that the prepared materials contain a large number of hydroxyl groups. The antisymmetric stretching vibration peak of Si-O-Si (1090.94 cm<sup>-1</sup>), the symmetric stretching vibration absorption peak of Si-O-Si (798.78 cm<sup>-1</sup>) and the antisymmetric bending vibration of O-Si-O (465.85 cm<sup>-1</sup>) are all obvious existence.

**The pore structure of DBPC:** Fig. 4 is the pore size distribution curve of diatomite based porous ceramics. It can be seen from the figure that the range of pore size of DBPC is 300~3500 nm. Because of the reservation of the larger original holes of diatomite, the pore size ranges from 300 nm to 800 nm is primary. The pore size over 800 nm are formed by the holes from the particle accumulation.

The detection results on the specific surface area, the mean pore diameter, the pore size distribution and the porosity of DBPC were measured by mercury intrusion method and given in Table 1. It can be seen from the table that the sample of DBPC has wide pore size distribution, larger spe-

Table 1: Pore size distribution, porosity and specific surface area of DBPC.

Specific surface area/m <sup>2</sup> ·g <sup>-1</sup>	Mean pore diameter/nm	Pore size distribution/nm	Porosity/%
6.14	1493.8	300~3500	47.8

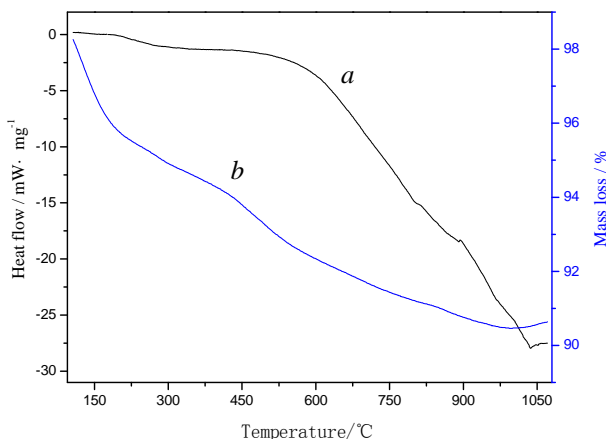


Fig. 1: DTA-TG curves of DBPC.

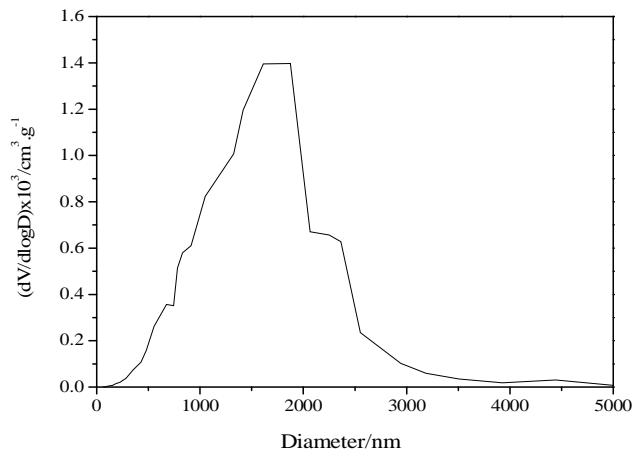


Fig. 4: Pore size distribution of DBPC.

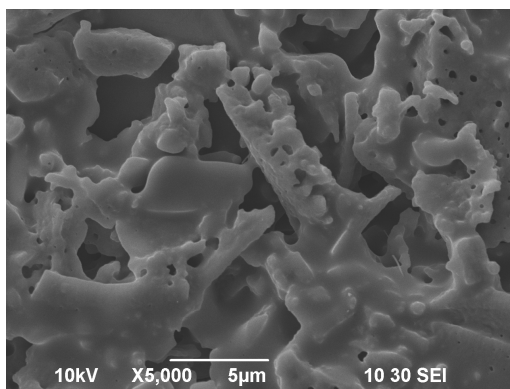


Fig. 2: SEM photograph of DBPC.

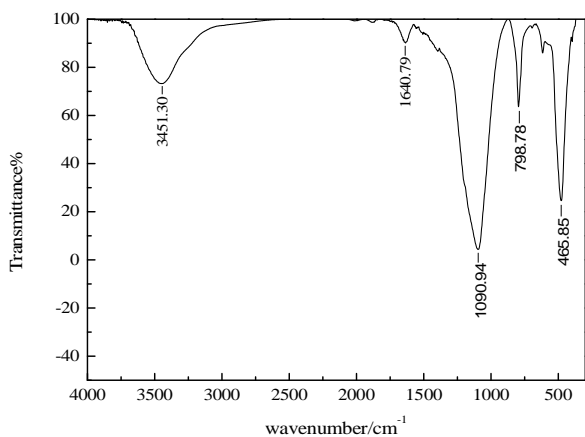


Fig. 3: FT-IR spectrum of DBPC.

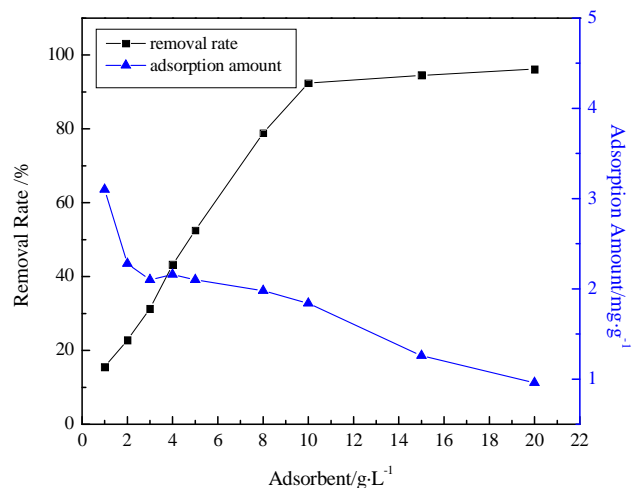


Fig. 5: Adsorption of Cu<sup>2+</sup> with different concentrations of adsorbent.

cific surface area and higher porosity. This characteristic makes the materials to have plenty of adsorption sites and be beneficial to the adsorption on the surface or in the pore passages of DBPC.

**The adsorption of DBPC on Cu<sup>2+</sup>:** Fig. 5 shows the the adsorption of Cu<sup>2+</sup> with the different adsorbent dosages. As can be seen from the figure, the removal rate of the copper ion increased with the increase of the dosage of DBPC, and the adsorption quantity was reduced gradually. Because of the increase of the adsorbent dosages providing more adsorption potential, this makes the removal rate to increase significantly. The rise of the removal rate brings about the Cu<sup>2+</sup> concentration to decrease in the solution. It follows that the relative adsorption rate declines, and the adsorption quantity of Cu<sup>2+</sup> decreases correspondingly in the same adsorbent. When the dosage of DBPC reaches 10 g/L, copper ion concentration reduces to 1.6 mg/L, and the removal rate achieves 92.5%. By increasing the adsorbent further, the removal rate of the copper ion does not increase. This is mainly because the increase of the adsorbent makes the repulsive force produced by the metal ions improve, the

free metal ions wanting to access further the depth and encounter the greater resistance. In the end, the adsorption and the resolving reach the relative balance.

On the other hand, there are a certain amounts of OH-, Si-O-Si and O-Si-O on the surface of DBPC. These groups have highly active unsaturated bonds. Hydroxyl groups OH- easily react with heavy metal ions in the solution to precipitate, or fix the heavy metal ions on the surface of DBPC through the ionic bonds (Murathan et al. 2005, Al-Ghouti 2004). This not only controls the surface properties such as surface activity, surface charge, water solubility and hydrophilic-to-hydrophilic etc., but also respond to the ligand (complex) - exchange reaction sites. This shows that the adsorbability of diatomite-based porous ceramics on  $\text{Cu}^{2+}$  is relatively great.

## CONCLUSIONS

With diatomite as the main material, using the means of wet grinding, rolling the ball shape and high-temperature calcinations, a new kind of environmental material—diatomite-based porous ceramics—with the pore size distribution from 300 nm to 3500 nm was produced. This material has the pore porosity of 47.8% and the specific surface area of 6.14  $\text{m}^2/\text{g}$ . There are a certain bonds such as OH-, Si-O-Si and O-Si-O on the surface of DBCP, which makes DBPC to have a good adsorption performance to pollutants. The removal rate on  $\text{Cu}^{2+}$  is up to 92.5%.

## ACKNOWLEDGEMENTS

The authors gratefully acknowledge the financial support

from the National Natural Science Foundation of China (No. 2013GGJS-088) and from Science and Technology Key Projects of Zhengzhou (No. 141PPTGG388).

## REFERENCES

- Al-Ghouti, M.A. 2004. Flow injection potentiometric stripping analysis for study of adsorption of heavy metal ions onto modified diatomite. *Chem. Eng. J.*, 104: 83-91.
- Annagiev, M.K., Bairamova, S.S. and Mamedov, Z.A. et al. 2012. Sorbents based on diatomite from Shemakha deposit for cleaning used compressor oils. *Chem. Technol. Fuels Oils.*, 48(1): 78-82.
- Chung, J.S. 1996. Deep-ocean mining? Technologies for manganese nodules and crusts. *Intern. J. Shore Polar Eng.*, 6(4): 244-254.
- Gao, R.Q., Zheng, S.L. and Liu, Y. et al. 2008. Preparation of diatomite-based porous ceramics and adsorption and degradation. *J. Chin. Ceram. Soc.*, 36(1): 22-24.
- Ivanov, S.É. and Belyakov, A.V. 2008. Diatomite and its applications. *Glass Ceram.*, 65(1-2): 48-51.
- Liu, J., Wang, H.L. and Lü, C.X. et al. 2013. Remove of heavy metals ( $\text{Cu}^{2+}$ ,  $\text{Pb}^{2+}$ ,  $\text{Zn}^{2+}$  and  $\text{Cd}^{2+}$ ) in water through modified diatomite. *Chem. Res. Chin. Univ.*, 29(3): 445-448.
- Murathan, A. and Benli, S. 2005. Removal of Cu super (2+), Pb super (2+) and Zn super (2+) from aqueous solutions on diatomite via adsorption in fixed bed. *Fresenius Environ. Bull.*, 14(6): 468-472.
- Simonenko, E.P., Simonenko, N.P. and Zharkov, M.A. et al. 2015. Preparation of high-porous SiC ceramics from polymeric composites based on diatomite powder. *J. Mater. Sci.*, 50(2): 733-744.
- Sun, C.Y., Tan, X. and Zhou, X.Y. et al. 2003. Ocean polymetallic nodules and crusts rich cobalt research review of mineral materials. *Metallic Ore Dressing Abroad*, 9: 4-11.
- Zheng, S.L., Sun, Z.M. and Hu, Z.B. et al. 2014. The processing and utilization of China diatomite resource and its development trend. *Earth Science Frontiers*, 21(5): 274-280.